Electronic Supplementary Information : Influence of lipid composition of model membranes on methacrylate antimicrobial polymer - membrane interactions

Upayan Baul[1, a)] and Satyavani Vemparala[2, b)]

[1)] *Department of Chemistry, The University of Texas at Austin, 105 E. 24th St., A5300, Austin, TX 78712-1224, USA*

[2)] *The Institute of Mathematical Sciences, C.I.T. Campus, Taramani, Chennai 600113, India*

[a)]Electronic mail: upayanb@utexas.edu

[b)]Electronic mail: vani@imsc.res.in

Initial equilibration of membrane systems

The starting configuration of all membranes were taken from pre-equilibrated membrane patches constructed using CHARMM-GUI's Membrane Builder module[1,2]. All membranes were adequately hydrated to 50 water molecules per lipid molecule, and Na^+ and Cl^- ions were added to set the salt concentration of the neutralized systems to 150 mM. At the initial stages of the simulations, the membranes were subjected to planar, harmonic, and dihedral restraints, which were gradually reduced to zero over 0.8 ns. Following the same, each membrane system was equilibrated for 50 ns, over which the energy, temperature, pressure and area per lipid were tested for convergence.

Calculation of lipid-packing defects and local bilayer thicknesses

The lipid-packing defects are identified separately for the individual bilayer leaflets. The plane of a bilayer leaflet is divided into $1\mathring{A} \times 1\mathring{A}$ grid cells. For each cell one can envisage a circular disc in the bilayer plane, with radius equal to half diagonal length ($\sim 0.7\mathring{A}$) and centered at the center of the grid cell. For every grid cell, the leaflet is scanned starting from the aqueous phase towards the bilayer center. The first bilayer atom to have a van der Waal overlap with the disc (computed using on-plane 2D separation between atom and grid cell centers) is identified. If the atom identified is a polar lipid head group atom, the cell is defined as *non-defect*. However, if the atom is an aliphatic one, its depth within the bilayer relative to the *sn-2* carbon of the nearest glycerol group is determined. If the atom is observed to reside more than $1\mathring{A}$ deeper within the bilayer relative to the *sn-2* carbon, the grid cell is defined as a *geometrical defect*, else as a *chemical defect*. Following the assignment of all grid cells for a leaflet, the clustering of the defect cells is computed using cluster multiple labeling technique due to Hoshen and Kopelman[3], taking into account the periodicity of the simulation box. The area corresponding to each cluster is obtained, which is binned to obtain the probability distributions of interfacial lipid packing defects as a function of defect surface area. It is important to note that geometrical defects are a sub-category of chemical defects, so in identifying the clusters of chemical defects, the geometrical defects are also included.

Local bilayer thickness was obtained using a similar grid-based Cartesian scheme. The

plane of the bilayer was divided into small grids ($2\mathring{A} \times 2\mathring{A}$). For a given system configuration and for each cell in the grid, phosphate groups were identified in the two leaflets that occupy the grid, or lie closest to it (in the plane parallel to the bilayer). Local bilayer thickness for the grid point can then be defined as the separation along bilayer normal between the identified phosphate groups in the two leaflets. The thickness distribution thus obtained was averaged over uncorrelated system configurations over the entire production run.

Comment on the influence of defect sites on the partitioning mechanism of polymers

Higher the exposure of the hydrophobic tail atoms, in terms of defects observed, higher is the individual polymer adsorption on the membrane surface. While the the charged groups of the polymers interact favorably with the charged head groups (PG lipid molecules) in all the membrane systems considered, the barrier to adsorb on the membrane surface may be dictated by the non-favorable interactions between the hydrophobic side arms of the polymers with the polar head groups. However, the existence of exposed hydrophobic lipid groups can provide an energetically favorable environment for the polymer hydrophobic arms in relative measure, reducing the energy barrier for the release of a polymer from the aggregate. Further, the increased ability to favorably interact with lipid atoms at the interface can lower the free energy barrier to partitioning through multiple correlated mechanisms.

It is well known that the ability to take up extended conformations at the interface favors ease of partitioning[4–6]. The defect sites help minimize the unfavorable exposure of hydrophobic groups, the prominent driving factor for compact polymer conformations. Participation of both charged and hydrophobic side arms in binding to lipid bilayer atoms can be envisaged to result in stronger and more stable binding. Furthermore, binding of hydrophobic polymer moieties to geometrical defects can also be of special importance in the subsequent reorganization of lipid head groups, further allowing the membrane partitioning of adsorbed polymers. Consistent with this view, in our study, the E4 polymers were observed to make favorable contacts with doPE-PG lipid head group atoms to a considerably greater degree than doPC-PG lipid head group atoms in their adsorbed, yet unpartitioned states. The membrane-bound conformations were also observed to be more extended with doPE-PG lipid membrane (as well as with dpPE-PG in the current simulations and poPE-

PG from our previously published results[7]) compared to doPC-PG (also from E4 dispersed - doPC-PG membrane system).

Supplementary figures

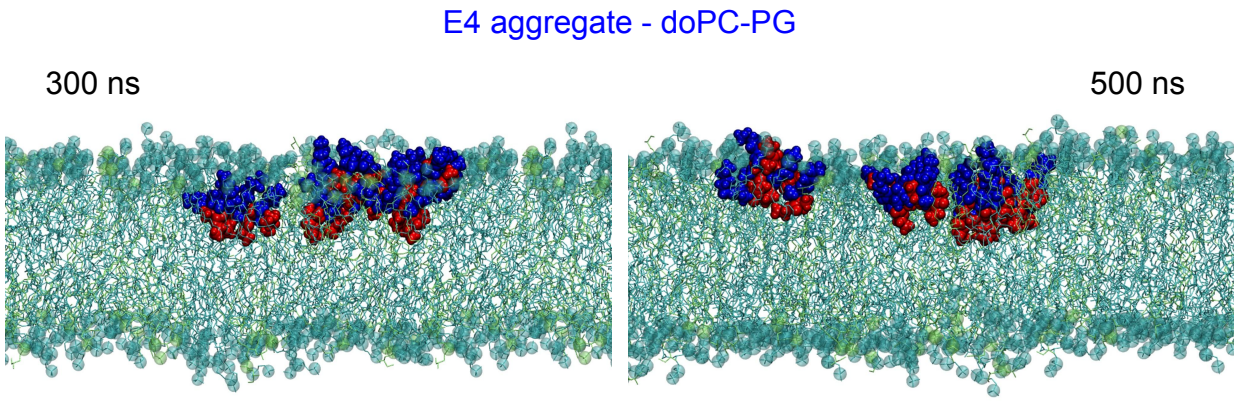

FIG. SI. Snapshots of E4 the aggregate - doPC-PG membrane system at the end of 300 ns and 500 ns of simulation. The snapshots show that the system conformations observed the end of 300 ns and 500 ns are visually similar. The notable change is that the aggregate is more loosely bound at the end of 500 ns.

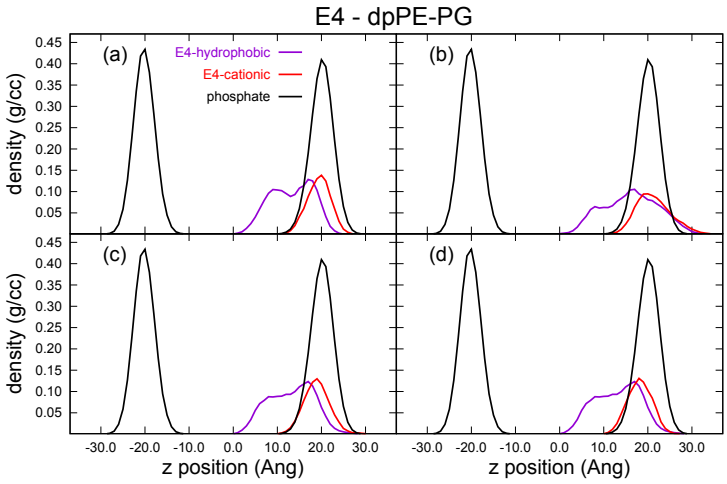

FIG. SII. Density profiles of E4 - dpPE-PG system components along the direction of membrane normal (z-axis). Each plot corresponds to one of the four E4 polymers in the simulated system. Plot (a) corresponds to the plot shown on Fig. 5(b) of the main article.

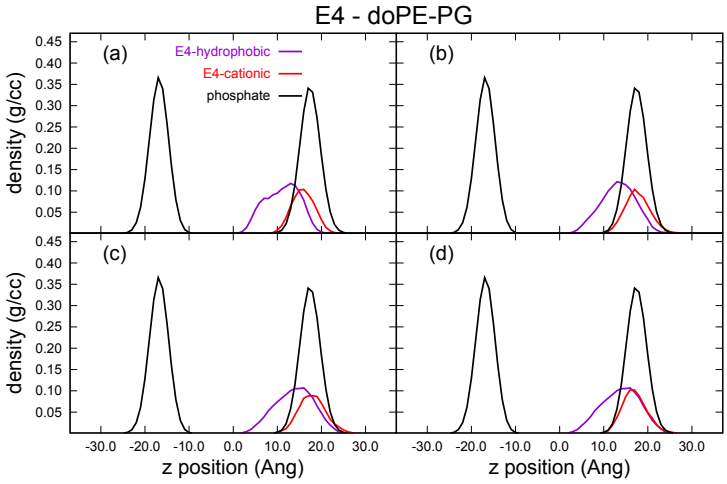

FIG. SIII. Density profiles of E4 - doPE-PG system components along the direction of membrane normal (z-axis). Each plot corresponds to one of the four E4 polymers in the simulated system. Plot (a) corresponds to the plot shown on Fig. 5(c) of the main article.

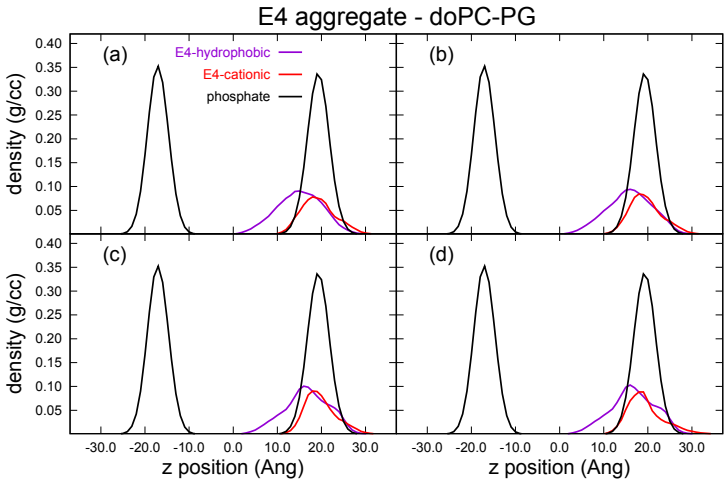

FIG. SIV. Density profiles of E4 aggregate - doPC-PG system components along the direction of membrane normal (z-axis). Each plot corresponds to one of the four E4 polymers in the simulated system. Plot (a) corresponds to the plot shown on Fig. 5(d) of the main article.

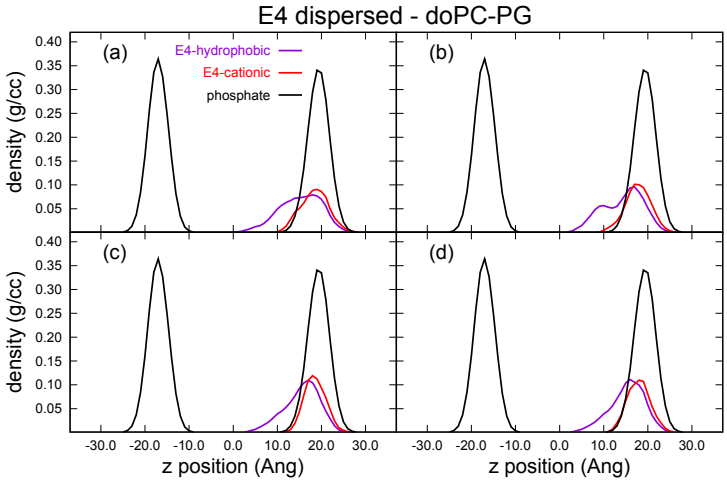

FIG. SV. Density profiles of E4 dispersed - doPC-PG system components along the direction of membrane normal (z-axis). Each plot corresponds to one of the four E4 polymers in the simulated system.

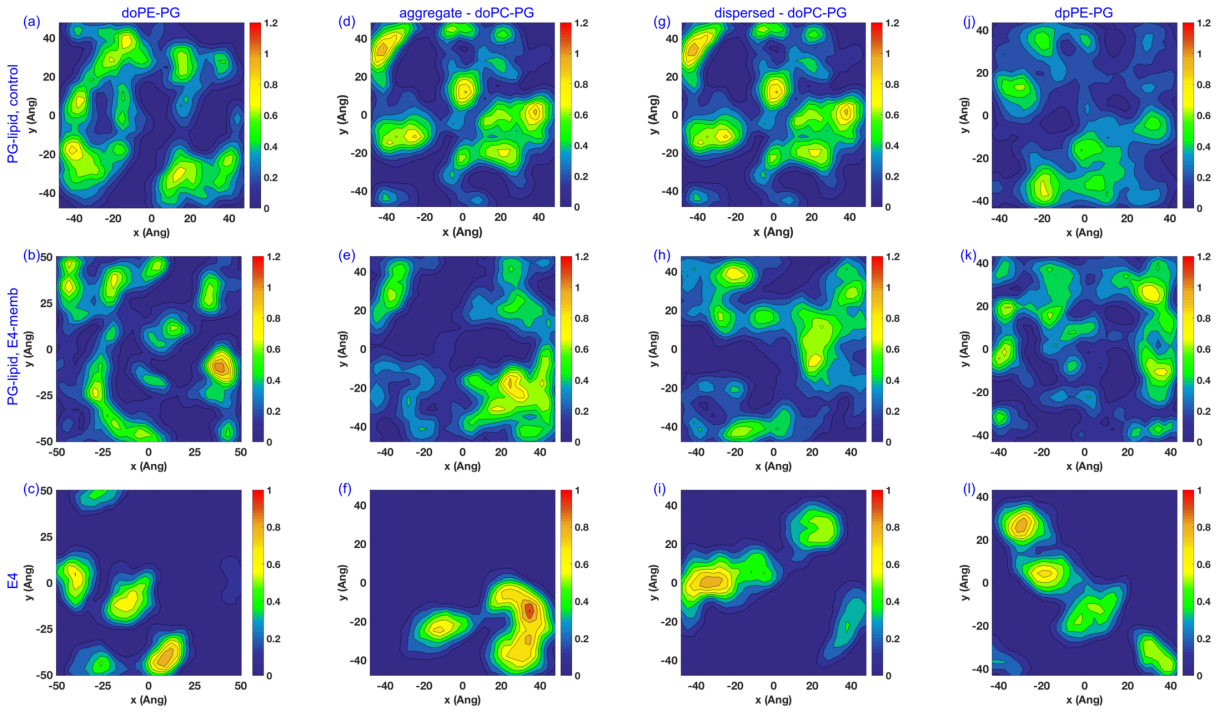

FIG. SVI. Contour plots showing the on-plane distributions of 2D number densities for the anionic (PG) lipid for control (top row) and E4 - membrane (middle row) systems. The bottom row shows the same for the E4 AMPoly atoms. Any appreciable demixing is only observed in (e), corresponding to the E4 aggregate - doPC-PG system. The same is accounted for by the localized (aggregated) presence of E4 AMPoly, whence the localization of DOPG lipids is electrostatics driven. Further, the same demixing was not observed to induce any appreciable changes in the local bilayer properties.

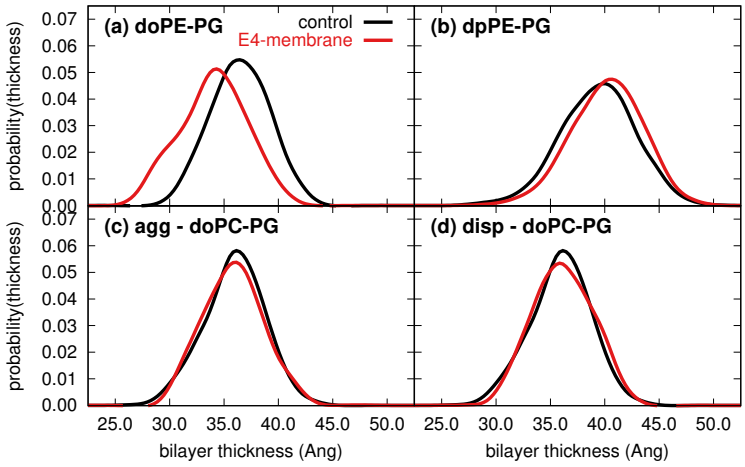

FIG. SVII. Probability distributions of overall local bilayer thicknesses. Plots for control and E4 - membrane systems are shown in black and red respectively. (a) and (b) clearly show the respective decrease and increase in bilayer thickness observed with the partitioning of E4 AMPoly, discussed in the main text. Figures (c) and (d) show that E4 AMPoly have no effects on doPC-PG bilayer thickness. Local bilayer thicknesses were obtained using a grid-based Cartesian scheme described in section 2 of the main text.

REFERENCES

[1]S. Jo, J. B. Lim, J. B. Klauda and W. Im, *Biophysical Journal*, 2009, **97**, 50 – 58.

[2] http://www.charmm-gui.org/?doc=input/membrane .

[3]J. Hoshen and R. Kopelman, *Physical Review B*, 1976, **14**, 3438–3445.

[4]K. A. Brogden, *Nature reviews. Microbiology*, 2005, **3**, 238–250.

[5]M. Zasloff, *Nature*, 2002, **415**, 389–395.

[6]E. F. Palermo, S. Vemparala and K. Kuroda, *Biomacromolecules*, 2012, **13**, 1632–1641.

[7]U. Baul, K. Kuroda and S. Vemparala, *The Journal of Chemical Physics*, 2014, **141**, 084902.